

The SHAlow RADar (SHARAD) Experiment, a subsurface sounding radar for MRO

R. Seu¹, D. Biccari¹, M. Cartacci¹, A. Cicchetti¹, O. Fuga¹, S. Giuppi¹, A. Masdea¹, R. Noschese¹, G. Picardi¹, C. Federico², A. Frigeri², P. T. Melacci³, R. Orosei⁴, R. Croci⁵, M. Guelfi⁵, D. Calabrese⁵, E. Zampolini⁵, L. Marinangeli⁶, E. Pettinelli⁷, E. Flamini⁸, and G. Vannaroni⁹

¹ Università di Roma “La Sapienza”, Dipartimento INFOCOM, Via Eudossiana 18, I-00184 Roma, Italy

² Università di Perugia, Dipartimento di Scienze della Terra, Piazza dell’Università 1, I-06123 Perugia, Italy

³ Università di Perugia, Dipartimento di Matematica e Informatica, Via Vanvitelli 1, I-06123 Perugia, Italy

⁴ Istituto Nazionale di Astrofisica, Istituto di Astrofisica Spaziale e Fisica Cosmica, Via del Fosso del Cavaliere 100, I-00133 Roma, Italy

⁵ Alcatel Alenia Space, Via Saccomuro 24, I-00131, Roma, Italy

⁶ Università “D’Annunzio”, Dipartimento di Scienze, International Research School of Planetary Sciences, Viale Pindaro 42, I-65127 Pescara, Italy

⁷ Università di Roma “Roma Tre”, Dipartimento di Fisica, Via della Vasca Navale 84, I-00146, Roma, Italy

⁸ Agenzia Spaziale Italiana, Viale Liegi 26, I-00198 Roma, Italy

⁹ Istituto Nazionale di Astrofisica, Istituto di Fisica dello Spazio Interplanetario, Via del Fosso del Cavaliere 100, I-00133 Roma, Italy
e-mail: robseu@infocom.uniroma1.it

Abstract. SHARAD (SHAlow RADar) is a radar for the study of the Martian subsurface provided by the Italian Space Agency (ASI) as a facility instrument on board NASA’s Mars Reconnaissance Orbiter 2005 spacecraft. The scientific objective of SHARAD is the detection of water, either liquid or solid, and the profiling of subsurface ice layers in the first hundreds of meters of the Martian subsurface. Although the Martian surface is not uniformly amenable to subsurface sounding, it will be possible to find favourable conditions for the achievement of scientific objectives. SHARAD is complementary to the Mars Advanced Radar for Subsurface and Ionosphere Sounding (MARSIS) experiment on board ESA’s Mars Express spacecraft, as it is capable of a better resolution (because of the wider transmitted bandwidth) at the cost of a reduced penetration (higher operating frequency). SHARAD benefits from MARSIS experience both for the modelling of the expected surface clutter, and for the inversion of echo data. Preliminary data acquired during the instrument commissioning period around Mars have demonstrated the correct working of the instrument.

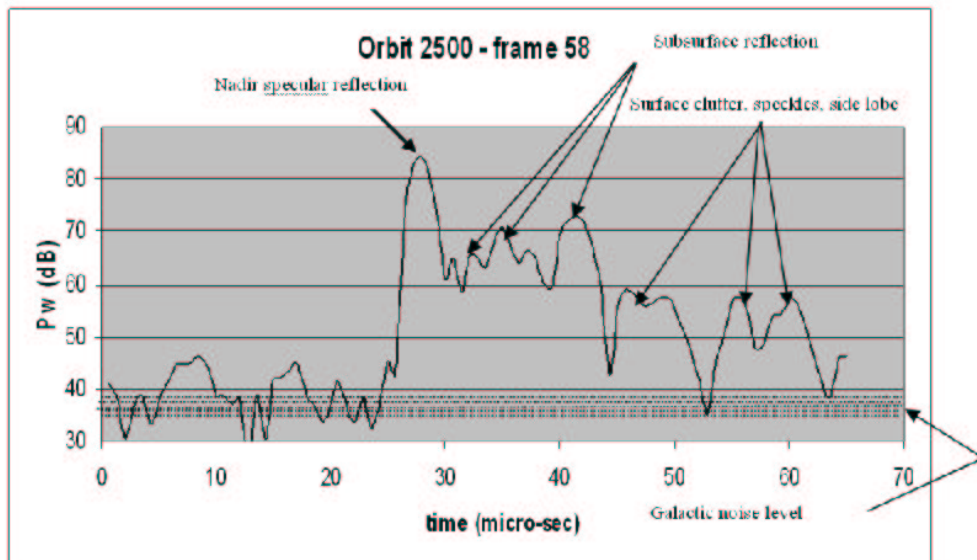


Fig. 1. Plot of an individual processed radar echo (or “frame”) from the MARSIS experiment. The horizontal axis is the time delay of the echo in μs , while the vertical axis is the echo power in dB. The main peak in the plot is the reflection produced by the Martian surface, while smaller subsequent peaks are subsurface reflections. Distant peaks (i.e. peaks reaching the radar 15 μs or more after the surface reflection) are lateral surface echoes, the so-called “clutter”.

Key words. Space vehicles: instruments – Techniques: radar astronomy – Planets and satellites: individual: Mars

1. Introduction

1.1. Experiment Overview

A sounding radar, SHARAD, is now in orbit around Mars, joining the MARSIS radar in the exploration of the Martian subsurface. SHARAD (SHALLOW RADAR) is a subsurface sounding radar provided by ASI (Agenzia Spaziale Italiana) as a facility instrument for NASA’s Mars Reconnaissance Orbiter (MRO) mission (Graf et al. 2005). It is designed to characterize electrically the upper several hundred meters of the Martian subsurface. In a nutshell, the SHARAD radar will emit EM waves from its 10 m dipole antenna, and they will reflect from the Martian surface as well as penetrate it. The waves transmitted into the interior will reflect from subsurface dielectric interfaces. The dipole antenna will collect some fraction of the energy reflected from both the Martian surface and subsurface reflectors, with the latter time-delayed from the former according to the wave velocity along the interior propagation path. A dielectric picture

Send offprint requests to: R. Seu

(a “radargram”) of the surface and subsurface is built up in one direction by time delay and in an orthogonal direction by motion of the MRO spacecraft along its orbit. The radargram is a sequence of frame of synthetic aperture. An example of a frame and a radargram obtained by the sounding radar MARSIS (Picardi et al. 2005), flying on the Mars Express spacecraft, is shown in Fig. 1 and Fig. 2.

The primary obstacle to the identification of subsurface echoes is the interference from off-nadir surface echoes (known as “surface clutter”) that arrive at the radar receiver with the same time delay as subsurface echoes. This obstacle can be mitigated by various technique; one method is to simulate the clutter from digital elevation models of surface topography. SHARAD operates with a 20 MHz center frequency and a 10 MHz bandwidth, which translates to a vertical resolution of 15 m in free-space and $15 / \sqrt{\epsilon}$ m in a medium of relative permittivity ϵ . The transmitted signal is a 10 W, 85 μ s chirped pulse. The voltage of the returned signal is recorded, and the pulse repetition frequency (PRF) over-samples the Doppler spectrum, allowing for coherent integration of pulses on-board the spacecraft, while still allowing for Doppler focusing in ground data processing. Indeed, except for on-board pre-summing, all of the data processing will take place on the ground, including range and Doppler focusing of the chirp signals, and calibration of the processed data. Data will be processed at the SHARAD Operations Center of Alcatel Alenia Spazio in Rome, Italy, under the guidance and control of the SHARAD science team. Data will be distributed to the community from ASDC (ASI Science Data Center) in Frascati, Italy, and from the Geosciences Node of the Planetary Data System at Washington University in St. Louis, USA (WUSTL-PDS).

1.2. Scientific Objectives

The primary objective of the SHARAD experiment is to map, in selected locales, dielectric interfaces to several hundred meters depth in the Martian subsurface and to interpret these results in terms of the occurrence and distribution of expected materials, including competent rock, soil, water and ice. This is a seemingly bland and cautious set of objectives, making no particular promises about the unique detection of any specific material (e.g., water). Nevertheless, the subsurface of Mars presents ample possibilities for dielectric contrasts. The dielectric constant is a strong function of rock density, so boundaries between material of different porosities are dielectric reflectors. This contrast could arise, for example, from sedimentary materials in contact with basaltic rock, with ice in contact with solid rock, or ice-saturated porous rock in contact with ice-free porous rock. These contrasts alone lead to a large variety of subsurface targets for SHARAD to map. Examples include subsurface mapping of the polar layered deposits, both their internal layers and contact with underlying bedrock, of the layering within sedimentary rock sequences, of buried impact craters in the northern lowlands, of buried channels, and of stratigraphy within lava flows.

2. Radar Sounding

2.1. Principles

A radar sounder generates a high-power pulse of RF energy, which is radiated by the antenna towards the Martian surface as shown in Fig. 3. As discussed in the Introduction, the Martian surface will then reflect some of the energy from the first surface towards the sounder. Some of the energy impinging on the surface will be transmitted to the subsurface and will then travel towards the next reflecting interface and undergo attenuation by the material. When this RF energy pulse encounters the second layer interface, some of it will be returned toward the sounder and some will be transmitted to the next layer. In principle, the returns from the subsurface

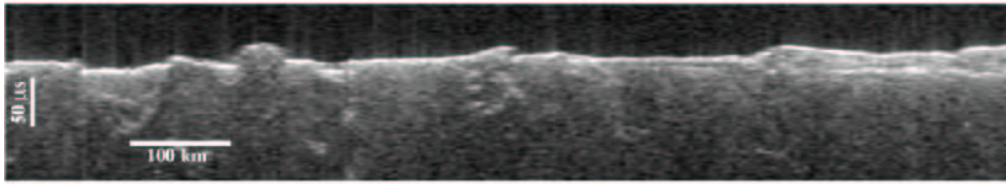


Fig. 2. A radargram produced using MARSIS frames acquired consecutively along the ground track of the Mars Express spacecraft. Each column of the image is an individual frame, as the one shown in Fig. 1, in which the radar echo power is color-coded in shades of gray, with brighter pixels corresponding to higher power levels. This method of displaying radar data results in an image representing a vertical section of the Martian subsurface along the spacecraft ground track. The structure of subsurface layers is discernible in the right part of the image.

should be much weaker than those of the surface. In actual application, in order to transmit enough energy from the antenna to the surface, the transmitted waveform must be spread over time. Subsequently it must be compressed in order to detect and isolate weak subsurface returns that are close to the strong first surface echo. This usage of a linear frequency modulated signal can produce side lobe problems that limit the subsurface detection capability of the radar. The first observed echo is the strong return from the surface, which then decays rapidly except for the effects of surface clutter. The strength of subsurface returns generally decreases as the depth of these echoes increases, until finally the signals are lost in a combination of surface clutter and/or cosmic noise. The detection of a specific subsurface feature is therefore dependent upon the strength of that particular subsurface return clearly rising above both the overall noise level of the system and the level of other surface returns arriving at the same time.

Therefore, to assess the expected performance of a Martian radar sounder, all of the following factors must be evaluated:

- the reflectivity of the surface and the subsurface as a function of the expected material composition and interface characteristics;
- the effect of the ionosphere – a Martian orbiting radar sounder operating at a frequency of few MHz can expect a significant drop in performance due to the ionosphere;
- the level of the galactic noise;
- the level of clutter echoes, which in turn are dependent on the surface topography.

The first surface reflection echoes of the sounder can be also processed to give estimates of the average height, roughness and reflection coefficient of the surface layer by using a classical altimetry approach (surface altimetry). The time delay of the echo makes it possible to estimate the average distance of the radar from a reference surface level (e.g., aeroid), while the duration of the waveform leading edge provides information about the large scale surface roughness averaged over the pulse-limited spatial resolution cell. Finally the peak value of the average echo waveform can be used to estimate the backscattering coefficient and, in conjunction with the roughness value, to estimate the Fresnel reflection coefficient of the surface.

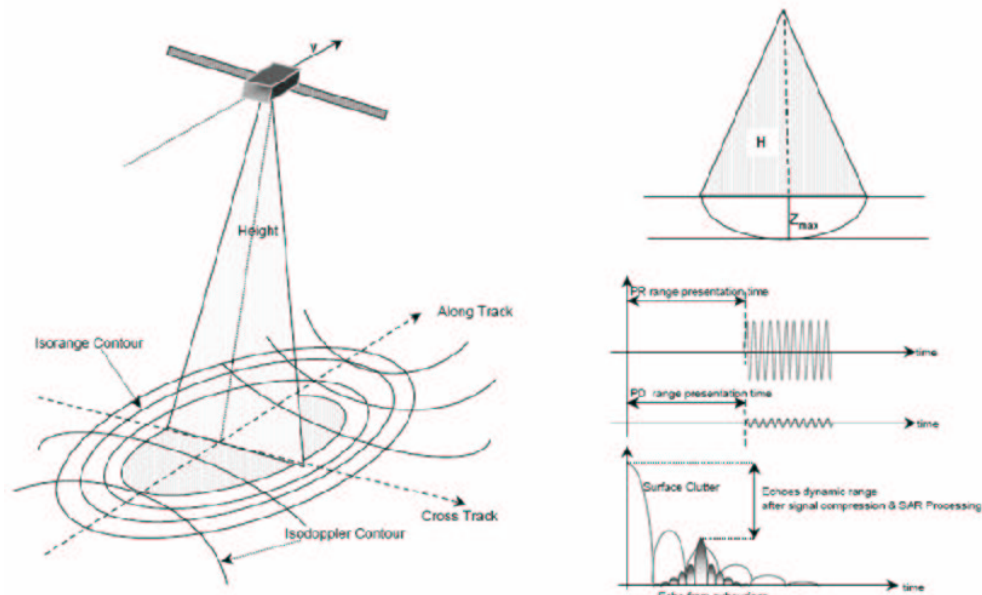


Fig. 3. Diagram illustrating some aspects of radar subsurface sounding from an orbiting spacecraft. See text for details.

2.2. SHARAD and MARSIS

SHARAD was preceded at Mars by a low-frequency radar sounder known as MARSIS, the Mars Advanced Radar for Subsurface and Ionospheric Sounding (Picardi et al. 2005), on the European Space Agency Mars Express orbiter. MARSIS was designed for maximum subsurface penetration depths, and thus uses frequencies as low as possible, given the Mars environment and the constraints of hardware implementation. For subsurface sounding, MARSIS utilizes four frequency bands, each of 1 MHz bandwidth, centered at 1.8, 3.0, 4.0 and 5.0 MHz. Data may be collected with any two of the four frequencies simultaneously. A 40 m long dipole antenna is used for both transmitting and receiving, while a second 7 m long monopole antenna is used for receiving only, as a means to identify and reject crosstrack topographic clutter. The 1 MHz instantaneous bandwidth provides a free-space range resolution of approximately 150 m. Lateral spatial resolution depends on surface roughness characteristics, but for most Mars surfaces the cross-track footprint is 10-30 km and the along-track footprint, narrowed by onboard synthetic aperture processing, is 5-10 km. Peak transmitted power out of the dipole antenna is ≈ 10 Watts. Coherent azimuth sums are performed onboard on ≈ 100 pulses taken at a PRF of 127 Hz, with a resulting signal-to-noise ratio for a typical Mars surface of 30-50 dB. A second mode is available for ionospheric sounding, using a series of pulses in frequency steps from 0.1 to 5.5 MHz. The MARSIS ionospheric or subsurface sounding signals will not reach the surface when the ionospheric plasma frequency is close to or above the sounding frequency.

The plasma frequency of the ionosphere, in absence of particular solar activity, is typically in the range of 0.5 to 5 MHz, with the higher values on the dayside. Thus the lowest (deepest penetrating) subsurface sounding frequencies can only be used on the nightside, while the higher frequencies are used mainly on the dayside. MARSIS and SHARAD are complementary in their

Table 1. Comparison of instrument and performance parameters between the MARSIS and SHARAD experiments.

	SHARAD	MARSIS
Frequency band	15-25 MHz chirp	1.3 - 2.3 MHz, 2.5 - 3.5 MHz, 3.5 - 4.5 MHz, 4.5 - 5.5 MHz chirps
Vertical resolution, theoretical, reciprocal bandwidth, $\epsilon = 4$	7.5 m	75 m
Transmitter power	10 W	10 W
Pulse length	85 μ s	250 or 30 μ s
Pulse repetition frequency	700 or 350 Hz	127 Hz
Antenna	10 m dipole	40 m dipole
Post-processor S/N	50-58 dB	30-50 dB
Horizontal resolution (along track \times cross track)	0.3 - 1 km \times 3 - 7 km	5 - 10 km \times 10 - 30 km

frequency ranges; MARSIS operates in the range of 1.3 - 5.5 MHz, compared with SHARAD at 15 - 25 MHz. Since most Mars materials are expected display increasing attenuation with frequency, the SHARAD signals are not expected to penetrate as deeply as those of MARSIS. However, in MARSIS observations of the Polar Layered Deposits (PLD), very little frequency dependence is seen, with the highest frequency bands penetrating just as deeply as the lower frequency bands. We expect that SHARAD will detect deeper interfaces within the PLD, and likely will penetrate to the base in all but perhaps the thickest (> 3 km) exposures. MARSIS has detected fine layering within the Southern Polar Layered Deposits (SPLD) (Plaut et al. 2005). The higher vertical resolution of SHARAD should allow discrimination of finer layering, providing additional insight into the compositional or physical variations responsible for the observed dielectric layering. Shallow (several 100s of m) interfaces have been detected by MARSIS in areas adjacent to the classical mapped SPLD (Plaut et al. 2005). These shallow deposits, likely ice-rich, are prime targets for SHARAD. In lower latitudes, MARSIS has detected shallow interfaces that should be detectable with SHARAD at better resolution. The detailed structure of the hypothesized shallowly-buried basin in Chyrsse Planitia (Picardi et al. 2005) may be revealed by SHARAD. SHARAD data may be useful in augmenting the inventory of buried impact features, as MARSIS has performed (Watters et al. 2005). The major contribution of SHARAD may well be that of a “fine-scale” stratigraphic mapper. A comparison of MARSIS and SHARAD performance is shown in Tab. 1.

3. Instrument description

SHARAD is composed of two main physical elements, the SEB (SHARAD Electronics Box) and the antenna. The SEB includes all of the transceiver electronics and the signal processing and control functions. It is made up of two separate electronic assemblies Receiver and Digital Section (RDS) and Transmitter and Front End (TFE) mounted on a support structure that acts as radiator for thermal control and includes the heaters and temperature sensors.

3.1. Transmitter/Front-End

The Transmitter and Front End Unit (TFE) is a self-standing component, devoted to amplifying the low level chirp signals coming from the Digital Electronic Section (DES) unit and coupling them to the dipole antenna; the unit also provides for the time division duplexing function, i.e., sharing the antenna between the transmitter and the receiver path.

3.2. Receiver

From an architectural point of view, SHARAD's receiver has been designed without the need for frequency-conversion; the receiver's front end performs a band-pass filtering function, while the received signal is amplified to a level sufficient for A/D conversion. The SHARAD receiver is based on a band-pass sampling technique, so the sampling rate can be much lower than that required by sampling at twice (or more) the highest frequency content of the bandpass signal. In fact, to satisfy Nyquist's theorem, the sampling rate must be at least twice the bandwidth of interest, not necessarily twice the highest frequency component. The choice of direct digitization of the RF input signal has, for this application, several advantages with respect to a frequency-conversion configured receiver. The most obvious reason is that a conversion mixer is not required. A built-in local oscillator for conversion is also not needed.

3.3. Digital subsystem

The Digital Electronics Section (DES) is the heart of SHARAD and contains many of the instrument functions, including command and control, low-power radar pulse generation, science data processing and formatting, and timing. The DES provides all the hardware and software components to enable SHARAD operations.

3.4. Antenna

The SHARAD antenna is a 10 m dipole made of two 5 m foldable tubes, which, in stowed configuration, are kept in place by a system of cradles and, when released, will self-deploy because of their elastic properties. Electrically, the antenna is fed at the center, interfacing the SEB by means of two wires (one for each dipole). The connected wires together form a balanced connection line. The line itself has no controlled impedance, (the antenna not having any matching network) and the load seen on the TFE side is therefore frequency dependant (thus requiring a dedicated matching network within the TFE).

4. SHARAD performance

4.1. Link analysis and Doppler focusing

The SHARAD instrument is designed to radiate 10 Watts to achieve a specular surface Signal-to-Noise Ratio (SNR) of 50.6 ± 1.25 dB. This is realized in the following way. The radar signal SNR depends on a number of factors and can be expressed as:

$$\text{SNR} = \frac{P_p G^2 \lambda^2 \Gamma}{64 \pi^2 R_0^2 K T_S B_N L} \quad (1)$$

where P_p is the transmitted power, G is the antenna gain, λ is the wavelength, Γ the surface power reflection coefficient, R_0 the distance from spacecraft to surface, T_S the limiting noise

temperature, K is Boltzmann's constant, B_N the noise bandwidth, and L the propagation loss. Additional signal power is subsequently obtained by range (G_r) and Doppler (G_a) focusing or gain. The range compression gain is the time-bandwidth product ($B\tau$) of the 10 MHz bandwidth and the 85 μ s chirp signal, that is 850 (29.3 dB). Because the chirp signal is weighted (nominally a Hanning function) to reduce range side lobes, the pulse compression is not ideal and loses up to 1.8 dB in compression gain. The present compression gain in range, G_r , is then taken as 27.5 dB. The azimuth (along-track) gain is assumed, conservatively, to be no larger than the coherent integration of signals returned in the first Fresnel zone. The spacecraft-to-surface distance, R_0 , can vary between 255 and 320 km over an MRO orbit. This leads to a Fresnel zone diameter D_{FZ} of

$$D_{FZ} = 2 \sqrt{\frac{\lambda R_0}{2}} = 2765 \text{ m} \div 3098 \text{ m} \quad (2)$$

The azimuth gain is given by

$$\begin{aligned} G_a &= \frac{L_{\text{syn}}}{\frac{V_{SC}}{\text{PRF}}} \\ &= \frac{2765 \text{ m} \div 3098 \text{ m}}{\frac{3400 \text{ m/s}}{\frac{1}{700}}} \\ &= 563 \div 633 \approx 28 \text{ dB} \end{aligned} \quad (3)$$

where V_{SC} is the spacecraft velocity and L_{syn} is the synthetic aperture length, taken as the diameter of the Fresnel zone. It has be highlighted that $1/\text{PRF}$ is the pulse repetition interval, PRI, in seconds, and thus it follows that:

$$G_a = \frac{L_{\text{syn}}}{\frac{V_{SC}}{\text{PRF}}} = \frac{L_{\text{syn}}}{L_p} \quad (4)$$

where L_p is the distance traveled by the spacecraft between pulses. So G_a can be interpreted simply as the number of pulses available for integration within a Fresnel zone. The realization of G_a is based on the premise that coherent integration can be performed for returned pulses from a ground patch of Fresnel-zone size. The focused signal-to-noise ratio, SNR_f , is then logarithmically given by the sum:

$$\begin{aligned} \text{SNR}_f &= \text{SNR} + G_r + G_a \\ &= -4.9 \pm 1.25 + 27.5 + 28 \\ &= 50.6 \pm 1.25 \text{ dB} \end{aligned} \quad (5)$$

The dynamic range for a subsurface-signal-to-noise ratio of 3 dB is then 47.6 ± 1.25 dB.

Based on this number, the penetration depth for different materials has been evaluated as a function of the radiated power. Synthetic aperture focusing can improve the along-track (azimuth) resolution without sacrificing the SNR. The azimuth spatial resolution, ρ_a , is approximately given by (300 km spacecraft altitude)

$$\rho_a \approx \frac{\lambda R_0}{2 D_{FZ}} = 750 \text{ m} \quad (6)$$

where for simplicity we have ignored the small difference between spacecraft and ground velocities. The azimuth focusing gain, C_a , is given approximately by:

$$C_a \approx \frac{2 D_{FZ}^2}{\lambda R_0} = 4 \quad (7)$$

which is of course the ratio of the ratio of the Fresnel zone diameter to the azimuth spatial resolution. The azimuth signal is highly oversampled by the 700 Hz PRF to avoid clutter folding. As long as the on-board coherent summing does not exceed the azimuth resolution, then there is no resolution degradation. The number of pulses N_{pulses} that could be summed in 750 m is thus

$$\begin{aligned} N_{\text{pulses}} &\approx \frac{\rho_a}{V_{SC}} \text{ PRF} \\ &= \frac{750 \text{ m}}{3400 \text{ m/s}} 700 \text{ Hz} \\ &\approx 150 \text{ pulses} \end{aligned} \quad (8)$$

The actual on-board pre-summing range is 1 to 32 samples (pulses), so this implies that even with the maximum amount of on-board pre-summing, additional coherent summing will have to be performed on the ground to achieve the full SNR. In Tab. 2 is shown the pre-summing pulses number and their impact on the data rate. Thus coherent summing can be done within a Doppler resolution cell on-board the spacecraft, and additional gain can be obtained by Doppler focusing on the ground to the desired azimuth resolution. The azimuth focusing process will by design integrate pulses that are over-sampled along the ground track for the realizable Doppler spectrum. Note that before pre-summing on board, a phase compensation with respect to the 20 MHz center frequency is carried out to compensate phase displacement due to the spacecraft radial velocity component and the surface slope. Information about these two quantities for specific data takes is uploaded to the spacecraft in the form of polynomial coefficients. The validity of this approach depends on local subsurface topographic variations being largely described by the local surface slope within a Fresnel zone. It is of course possible to construct longer synthetic aperture lengths, and thus obtain finer azimuth resolution, for rougher surfaces that provide backscatter beyond a Fresnel zone distance of spacecraft motion. This could reduce surface clutter, particularly from compact scatterers. If a subsurface reflector is relatively smooth in this case, then the improved azimuth resolution would not be realized for the subsurface feature, but the subsurface-to-surface-scatterer ratio should increase.

5. Instrument calibration

Two requirements for SHARAD instrument calibration are meaningful: the relative and absolute calibration. The relative calibration goal for SHARAD is derived from the primary science objectives. For example, mapping the distribution of water/brine and ice requires comparison of data collected at widely different locations on the Mars surface, and thus a degree of stability in stated power for the processed radar data is required. Given a hypothetical layer of brine at some fixed depth, we should be able to correlate observations of the interface at a range of observing latitudes. If all other factors (attenuation, surface roughness, etc.) were constant, we would wish to characterize the effective reflection coefficient of this interface to within about 30%. This corresponds to a relative calibration accuracy of ≈ 2 dB. For the absolute calibration of subsurface reflections, there is no requirement for SHARAD due to the model-dependent estimates of surface reflectivity, attenuation in subsurface layers, etc. However, calibration of absolute power

Table 2. Data production rate of the SHARAD instrument as a function of the number of bits per echo sample and of the number of echoes pre-summed on board.

Pre-summed pulses	Data rates (Mbps)		
	4 bits per sample	6 bits per sample	8 bits per sample
1	10.08	15.12	20.16
2	5.05	7.56	10.08
4	2.52	3.78	5.05
8	1.26	1.89	2.52
16	0.63	0.95	1.26
28	0.36	0.54	0.72
32	0.32	0.47	0.63

returned from the surface is possible by effectively inverting the radar equation for the scattering cross section of the surface. Further assumptions are necessary of course to obtain a Fresnel reflection coefficient, but these can be minimized over a flat, smooth surface. A reasonable target for the absolute calibration is ± 4 dB, assumed to be a good trade-off between scientific requirements and feasibility. In order to obtain a good result, calibration of the instrument was performed on the ground and will be performed again in flight during the transition and operations phases.

6. SHARAD science

There are a vast number of subsurface targets for SHARAD, some based on a knowledge of Mars geology, and others based on MARSIS results. Besides extensive spatial coverage of the polar regions, the SHARAD experiment will build up a time series ($L_s = 18$) by repeated sampling over 13 ground tracks, equally spaced in longitude over both poles. The objectives are to monitor the change in surface reflection coefficient as a function of season and locale, and to examine the seasonal dependence of the exploration depth of the radar. The first point is the concept that SHARAD can be used to monitor the comings and goings of seasonal deposits. To that end, there will be simultaneous observations by CRISM in its hyperspectral central scan mode.

7. Concluding remarks

The SHARAD instrument will be the second sounding radar to operate in orbit around Mars. The MARSIS radar on Mars Express was designed for deep penetration with relatively coarse resolution, while the SHARAD radar should have relatively less penetration, but an order of magnitude improvement in vertical resolution and nearly that in horizontal resolution. In contrast to MARSIS, essentially all of the SHARAD data processing will be on the ground, which allows flexibility in processing parameters and optimization for specific targets. MARSIS has already been successful in penetrating both polar caps to the underlying basement, in mapping interfaces within the polar layered terrain, and in mapping buried craters in the northern lowlands. Orbital sounding radars work well at Mars. Because of its superior vertical resolution, SHARAD's forte may well be that of a stratigraphic mapper, revealing more detail in the polar layered deposits, but also adding the third dimension to the knowledge of the structure of sedimentary layers observed at many places on Mars. All indications are that the instrument will operate as designed, and EMI will have an insignificant effect on data quality.

The antenna has been deployed on 17 September and several frame have been collected and processed and are under evaluation. The biggest challenge to data interpretation will be from the interfering effects of surface clutter as shown in a frame from MARSIS in Fig. 1.

References

- Graf, J. E. et al. 2005, *Acta Astronautica*, 57, 566
Picardi, G. et al. 2005, *Science*, 310, 1925
Plaut, J. J. et al. 2006, 37th Annual Lunar and Planetary Science Conference, abstract no.1212
Watters, T. R. et al. 2006, 37th Annual Lunar and Planetary Science Conference, abstract no. 1693